N_i = number of moles of substance per unit volume; R = reflectance; S = sensitivity; t = thickness; α_0 = incident coupling angle; ε = dielectric constant; ω = frequency.

See also: **Biochemical Applications of Fluorescence Spectroscopy; Biomacromolecular Applications of UV-Visible Absorption Spectroscopy; Chiroptical Spectroscopy, General Theory; Chiroptical Spectroscopy, Orientated Molecules and Anisotropic Systems; Ellipsometry; Surface Plasmon Resonance, Instrumentation; Surface Plasmon Resonance, Theory; Surface-enhanced Raman Scattering (SERS), Applications.**

Further reading

Garland PB (1996) Optical evanescent wave methods for the study of biomolecular interactions. *Quarterly Reviews of Biophysics* **29**: 91–117.

Harrick NJ (1967) *Internal Reflection Spectroscopy*. New York: Interscience.

Kovacs G (1982) Optical excitation of surface plasmon-polaritons in layered media. In: Boardman AD (ed) *Electromagnetic Surface Modes*, pp. 143–200. New York: Wiley.

Macleod AH (1986) *Thin Film Optical Filters*. Bristol, U.K.: Adam Hilger.

Raether H (1977) Surface plasma oscillations and their applications. *In*: Hass G, Francombe M and Hoffman R (eds) *Physics of Thin Films*, 9, pp. 145–261. New York: Academic Press.

Salamon Z and Tollin G (1998) Surface plasmon spectroscopy: A new biophysical tool for probing membrane structure and function. *In*: Chapman D and Haris P (eds) *Biomembrane Structure*. Amsterdam: IOS Press.

Salamon Z, Macleod AH and Tollin G (1997) Surface plasmon spectroscopy as a tool for investigating the biochemical and biophysical properties of membrane protein systems. II: Applications to biological systems. *Biochimica et Biophysica Acta* **1331**: 131–152.

Salamon Z, Macleod AH and Tollin G (1997) Coupled plasmon-waveguide resonators: A new spectroscopic tool for probing proteolipid film structure and properties. *Biophysical Journal* **73**: 2791–2797.

Salamon Z, Brown MF and Tollin G (1999) Plasmon resonance spectroscopy: probing molecular interactions with membranes. *Trends in Biochemical Sciences* **24**: 213–219.

Wedford K (1991) Surface plasmon-polaritons and their uses. *Optical and Quantum Electronics* **23**: 1–27.

Surface Plasmon Resonance, Instrumentation

RPH Kooyman, University of Twente, Enschede, The Netherlands

SPATIALLY RESOLVED SPECTROSCOPIC ANALYSIS
Methods & Instrumentation

In view of its simple instrumentation and its high surface sensitivity, surface plasmon resonance (SPR) and, more recently, SPR microscopy gains an increasing significance to numerous problems concerned with the study of interactions occurring near to or at surfaces. Applications can be found in the optical behaviour of metals, the study of Langmuir–Blodgett films and self-assembled monolayers, the interactions of proteins with interfaces, or redox reactions at interfaces. A fast-increasing field is the development of sensitive chemooptical sensors, intended to quantitatively and selectively monitor the presence of prespecified and chemical species, which can be in the range from a molecular mass of ~200 Da to 150 kDa. The main reason for the high sensitivity of SPR to surface phenomena should be attributed to the high local electromagnetic field strengths brought about by surface plasmons (SPs).

Several excellent monographs have been published on SPR theory, whereas an overview on applications is the subject of another article in this Encyclopedia. This chapter will be concerned with experimental techniques for a variety of SPR applications.

Basic requirements

Although SPs can be excited in an electron beam we will only consider the common case where they are generated by means of light.

SPs can be excited in any material where free charge carriers exist; in the majority of practical cases this means that a metal layer deposited on a

dielectric material is used as a medium to carry SPs. It turns out that the particular SP properties strongly depend on the nature of this deposited layer: if the metal is present as an island-like structure with patches of the order of a few tens of a nm, *radiative* plasmons will be excited resulting in large enhancements of the applied (optical) field strengths. This effect is mainly used to enhance surface responses in vibrational spectroscopy, such as Raman and infrared spectroscopy. *Nonradiative* SPs can be excited if the metal layer is applied as a thin (~50 nm) homogeneous layer. These plasmons have the peculiar property that the associated electromagnetic field is evanescent in character, i.e. the wave vector k_x parallel to the interface is (partly) real, whereas that perpendicular to the interface is imaginary. The generation of SPs is an elastic scattering process, implying that both energy and momentum are conserved. Consider the system as depicted in **Figure 1A**, where a metal layer is sandwiched between two media a and p, which is the commonly used Kretschmann configuration. In view of Snell's law, which states that through this whole system k_x remains constant, this has the consequence that SPs can only be excited at the interface a/m when light enters the metal layer through another interface m/p, *under the condition that* $\varepsilon_p > \varepsilon_a$, where ε_p, ε_a denote the respective dielectric constants. This is further illustrated in **Figure 1B** where the two lines a and p represent the light dispersion relations in the media a and p, respectively, and the curve represents the SP dispersion relation. A further necessary condition is that the exciting light has to be p-polarized, because light polarized along the metal interface cannot exist.

This short theoretical description contains all the information needed for setting up a basic SPR experiment.

Choice of metal support

An approximate expression for the SPR wave vector can be found in the literature:

$$k_x = (2\pi/\lambda)(\varepsilon_m \cdot \varepsilon_a/(\varepsilon_a + \varepsilon_m)^{1/2}) \qquad [1]$$

where λ is the wavelength *in vacuo*, and ε_m is the metal dielectric constant at the wavelength used. Generally, k_x of the incoming light can be adapted to that required by Equation [1] by inclining the beam relative to the interface normal. The following relation holds (see also **Figure 1A**):

$$k_x = (2\pi/\lambda) \cdot \varepsilon_p^{1/2} \cdot \sin\theta \qquad [2]$$

However, in practice the maximum angle θ that can be chosen is around 80°, implying that in a number of cases the dielectric constant of the support, ε_p, has to be selected such that within this material a light beam can have a *practical* k_x matching that of Equation [1]. If medium a is a water solution (refractive index $n_a \sim 1.33$; note that $n = \varepsilon^{1/2}$) then BK7 glass ($n_p \sim 1.52$) is an appropriate material. For media with higher refractive index SF10 glass ($n_p \sim 1.7$) can be used. (The abbreviations BK7 and SF10 refer to a nomenclature common in lens-making technology.) Convenient shapes of the dielectric support are prisms with apex angle 60 degrees or hemicylinders, which minimize the reflection loss of light when entering the support (cf. **Figure 1A**).

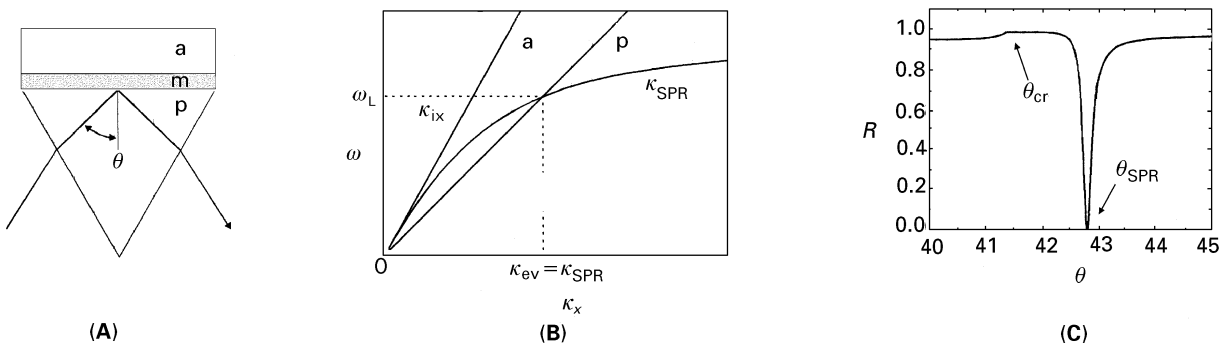

Figure 1 The SPR experiment. (A) a metal layer m is sandwiched between two dielectric media a and p. The direction *x* is defined parallel to the layer structure; (B) dispersion relation of SPs; see text; (C) a typical SPR curve when medium a has a refractive index $n_a = 1$. The angle θ_{cr} corresponds to the critical angle for the a/p interface.

Choice of metal layer

A typical application of SPR spectroscopy is to monitor a layer growth on the metal layer. Such a process can be modelled as a changing ε_a, which experimentally translates into a changing resonance angle θ_{SPR}. **Figure 1C** depicts a reflectance curve obtained from a SPR experiment. From the figure it is clear that in order to obtain maximum sensitivity to variation in ε_a the slope $dR/d\theta$ has to be as large as possible. For a given ε_a this depends in a complicated way both on the value of $\varepsilon_m(\lambda)$ and on the thickness of the metal layer. Generally, it can be said that smaller real and imaginary parts, $\mathrm{Re}(\varepsilon_m)$ and $\mathrm{Im}(\varepsilon_m)$, result in smaller resonance halfwidths, whereas the metal layer thickness is an important parameter determining the minimum reflectance. From **Table 1**, which gives an impression of $\varepsilon_m(\lambda)$ for some metals, it can be concluded that in the visible wavelength range silver is expected to exhibit the narrowest resonances. This is indeed found experimentally; however, in many situations where experiments are performed in a water or air environment, silver tends to undergo unwanted interactions with its environment, making this a less attractive material. In this respect gold is a much more stable material and thus this material has become the standard metal for SPR purposes, despite its resonance width that at $\lambda = 633$ nm is approximately three times larger than that of silver.

For a given metal the optimum layer thickness depends on the wavelength used, as illustrated in **Figure 2**; also the remarks on the importance of the value of $\varepsilon_m(\lambda)$ are apparent from the figure. For any wavelength within the visible range a gold or silver layer thickness can be found corresponding to a vanishing minimum reflectance; for the often used helium-neon laser wavelength $\lambda = 633$ nm this is approximately 47 nm for gold and 49 nm for silver.

Practical aspects As already mentioned, in order to be able to excite nonradiative SPs it is important to have available smooth, homogeneous metal layers with a well-defined layer thickness. An appropriate way to prepare these is to sputter or to evaporate the metal at a high rate ($\sim$1 nm s^{-1}) in a vacuum chamber (10^{-6} mbar) on the substrate of choice. In order to increase the adhesion between metal and underlying dielectric, the support is often precoated with a 2 nm Ti or Cr layer. It is not mandatory to coat directly on the prism; alternatively, a flat substrate, such as a microscope glass cover slip, can be used as a substrate. After coating, this plate is optically connected to the prism using a matching oil; care has to be taken that, in order to avoid spurious reflections, plate, oil and prism have the same refractive index in the wavelength region of interest.

Although a simple incandescent light source can be used for SPR, the use of a small HeNe or diode laser is far more convenient, in view of their well-defined wavelength and high degree of collimation.

Table 1 Real and imaginary parts of dielectric constant for some metals

Metal	*λ (nm)*	ε_{re}	ε_{im}
Aluminium	600	–29.8	7
	700	–46.6	22
	900	–55.5	30
Silver	500	–8.23	0.3
	700	–21.3	0.7
	900	–38.7	1.3
Gold	600	–8.37	1.2
	750	–18.2	1.2
	900	–28.5	1.8

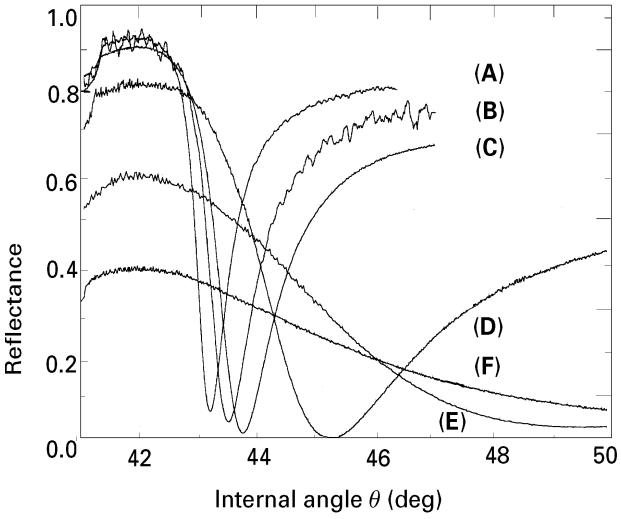

Figure 2 SPR reflectance curves for a bare gold layer with thickness 44 nm, measured with different wavelengths: (A) 676 nm; (B) 647 nm; (C) 633 nm; (D) 568 nm; (E) 514 nm; (F) 488 nm.

SPR instrumentation

Rotation stage

The most straightforward method to measure SPs is depicted in **Figure 3**, where the prism/gold assembly is placed on top of a rotation stage (angular resolution typically 0.01 degree). With such an arrangement, all the features of a SPR curve can be accurately determined. The light detectors consists of simple large area photodiodes whose output is fed into a low-noise current-to-voltage amplifier. The excitation laser beam is polarized such that both s- and p-polarized light enter the prism. The use of a

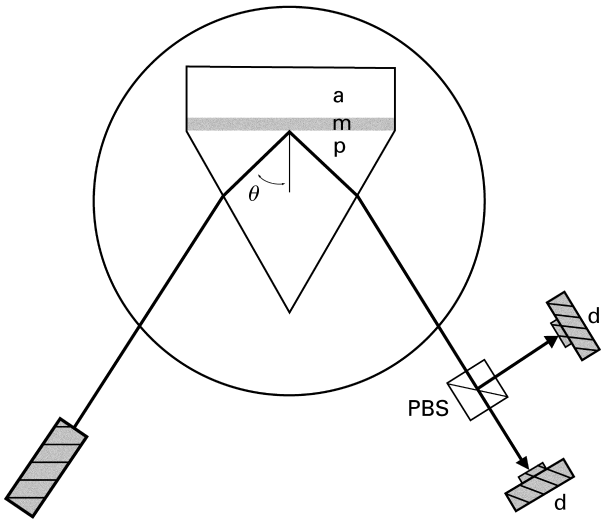

Figure 3 Rotation stage SPR setup. d: detectors; PBS; polarizing beamsplitter.

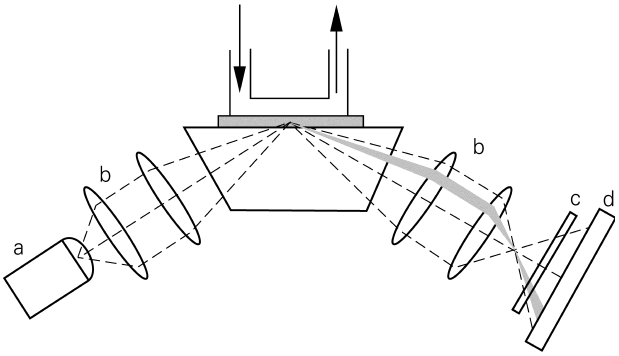

Figure 4 Use of focused beam. a: laser diode; b: focusing optics; c: neutral density filter; d: diode array. A flow cuvette is placed on top of the metal layer. Reproduced with permission from Sjölander S (1991) *Analytical Chemistry* **63**: 2338. © American Chemical Society.

polarizing beamsplitter serves two purposes: one detector measures only the reflected s-polarized light whose intensity is only affected by laser intensity fluctuations and angular dependent refraction losses, whereas the other detector in addition measures SPR effects. The ratio between the two outputs then provides a signal proportional to the net SPR response. In order to obtain an absolute angular read-out with sufficient accuracy the critical angle can be measured; this angle is very accurately known for a certain $\varepsilon_p/\varepsilon_a$ interface, and is an easily discernible feature in a SPR curve (cf. **Figure 1C**).

The obvious disadvantage of this setup is that it is difficult to monitor fast changes in the SPR curve. To be able to monitor time-dependent changes, the orientation of the rotation stage relative to the light beam is often set such that the reflectance is about halfway between maximum and minimum. A changing ε_a is then approximately linear in the monitored changed reflectance. However, one has to assume that a change of ε_a leaves the width of the SPR curve unchanged.

Use of a focused beam

A more elaborate setup is shown in **Figure 4**. Here, SPs are excited by a focused diode laser beam such that the beam waist is slightly displaced from the top metal/dielectric interface. In this way, a certain distribution of angles is present at the interface. The reflected beam is imaged onto an array consisting of a large number (50–100) of photodiodes. The angular range corresponding to resonance will exhibit a low intensity; consequently, the output of the diode array is a measure of the angular dependent reflectance. Although the distance between individual diodes is relatively large (~ 20 μm) the use of numerical interpolation techniques makes it possible to obtain an angular resolution of ~ 1 millidegree. Because no moving parts are involved, this system is capable of monitoring relatively fast-changing SPR characteristics: the temporal resolution will now be determined by the read-out rate of the diode array. A drawback of this system is that obtaining an *absolute* angular read-out is not as straightforward as in the case of the rotation stage, in view of the limited angular range that is applied to the metal/dielectric interface.

Photothermal detection

When a nonradiative SP decays it generates heat at the metal/dielectric interface. This observation can be fruitfully exploited to detect the presence of SPs. In a *photoacoustic* approach, the prism/metal assembly is placed in an airtight chamber. SPs are excited with an intensity-modulated light beam; the resulting periodic heat flow from metal to dielectric as a result of plasmon decay causes a periodic pressure variation in the dielectric which can be detected by a microphone in the sample chamber. A significant difference as compared with optical detection is that SPR is now detected as a *maximum* in response. This method is mainly used in fundamental studies where one is interested in SP decay. The method is less suited in situations where the dielectric of interest consists of a fluid, such as water.

In a related approach, the heat flow is detected optically (*photothermal deflection spectroscopy*). A representative setup is shown in **Figure 5**. The prism/metal assembly is placed upon a rotation stage, and SPs are excited in the usual way. Heat

produced by the decaying plasmon results in a gradient of the refractive index immediately above the metal layer. Consequently, the propagation direction of the light beam of the probe laser will be deflected and this can be measured, e.g. by using a position-sensitive detector. By modulating the SPR excitation beam and synchronous detection of the detector output, a differential signal is obtained whose angular dependence is directly related to the SPR curve. Using a HeNe laser as the excitation source an angular resolution of ~0.01 degree can be obtained; contrary to the setups where the reflectance is measured, this resolution can be improved by employing higher laser powers. It has been demonstrated that this deflection method is also useful in water solutions.

Sensor configurations

As already mentioned, an important application of SPR is in the field of chemical sensors. Such a SPR sensor system should be simple, compact, and relatively inexpensive, while retaining the angular sensitivity. Some representative SPR sensor systems will now be discussed.

Vibrating mirror device In the system as depicted in **Figure 6** the angle under which the light from a laser diode enters the interface is made time-dependent by means of a mirror, vibrating at a frequency of ~50 Hz. If the optical system in the excitation path is designed properly, the light spot during an angular scan of ~5 degrees is stationary on the interface to within 0.2 mm, while the beam divergence is kept within 0.02 degrees. Although this setup can be used to monitor the complete SPR curve, it is dedicated to determine only the angle of minimum reflectance θ_{SPR}, which for the majority of SPR applications is the main parameter of interest. This can be conveniently accomplished as follows: during one cycle of the vibrating mirror the beam traverses the reflectance minimum twice. The time span Δt between these two minimum is measured using appropriate electronics. If θ_{SPR} changes, Δt changes accordingly.

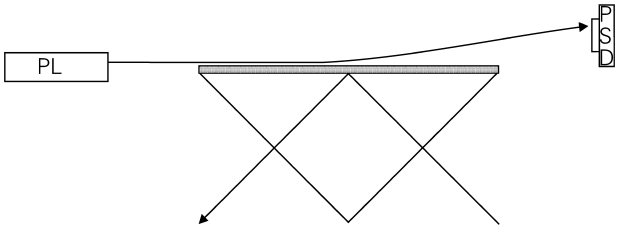

Figure 5 Basic photothermal detection setup. The position of the deflected beam of a probe laser PL is measured by a position-sensitive detector PSD.

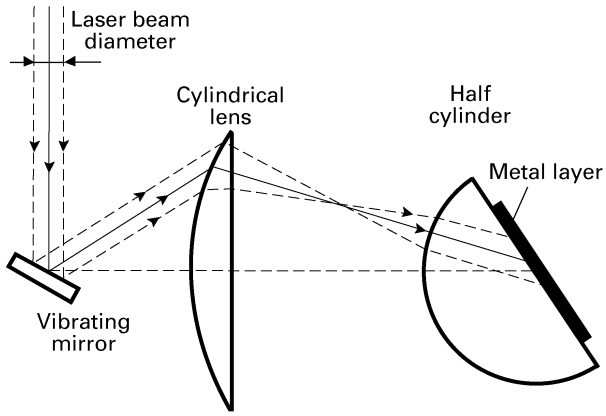

Figure 6 Vibrating mirror setup. a: vibrating mirror; b: cylindrical lens. Reproduced with permission from Lenferink ATM (1991) *Sensors and Actuators B (Chemical)* **3**: 261. Copyright 1991, with kind permission from Elsevier Science Ltd, The Boulevard, Langford Lane, Kidlington, OX5 1GB, UK.

Connected to a personal computer, this provides a versatile means to detect a SPR minimum with an angular resolution of 1 millidegree. The time resolution of such a setup will be determined by the vibration frequency of the mirror. (Note that vibrating mirrors operating at frequencies up to 10 kHz are available). For some applications the difficulty of obtaining an absolute angular read-out will be a disadvantage.

Use of diffraction-gratings In the foregoing configurations a SP was excited using a prism. However, plasmons can also directly be produced on a grating surface coated with a thin metal layer. The condition for SPR to occur is determined by the grating periodicity (typical value 2000 lines mm^{-1}) and the angle of incidence of the light beam, whereas the value of the reflectance minimum is solely determined by the grating depth (optimum value ~50 nm). Any of the above described setups can be used to detect SPs in this configuration. An advantage of this approach is that gold-coated gratings can be very easily and inexpensively manufactured as disposable replicas, once a holographic master grating has been produced. An important disadvantage is that the light beam has to enter the dielectric/metal interface from the dielectric side, implying that this is only a valuable approach for transparent media.

Fibre-optic devices In situations where the sensing surface should be remote from the signal processing equipment (such as in a hostile environment or in a living organism) the use of optical fibres can provide a practical solution. Apart from the trivial use of a fibre to transport the light to and from a separate

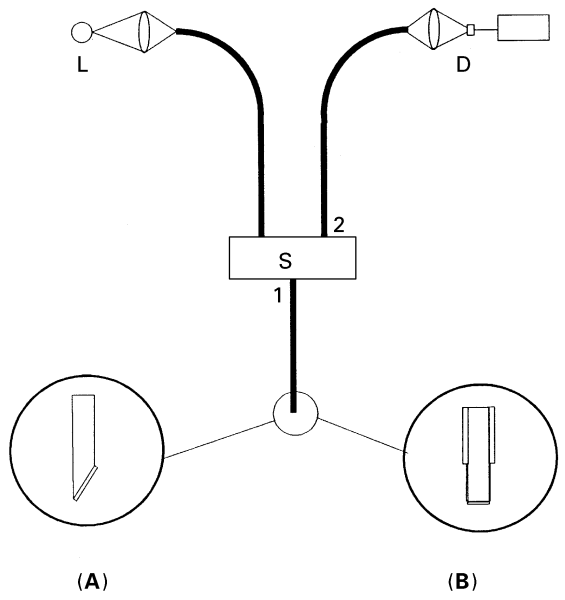

Figure 7 Use of fibre optics. L: light source; D: detector; S: fibre splitter/combiner; 1, 2: output ports. (A): single mode fibre; (B): multimode fibre (cf. text).

prism/metal assembly, it has also been demonstrated that the fibre can also be used as an *intrinsic* sensing interface, where part of the fibre surface replaces the prism. This concept is schematically shown in **Figure 7**. Light is fed into a fibre connected to an optical splitter/combiner S. The output port 1 of S is connected to a probe fibre, which is decladded at the distal end. After interaction with this end interface (see below) the light is reflected and again enters S, where it is transmitted to output port 2. A fibre connected to this port transports the light to a detector.

Several possibilities exist for the design of the decladded fibre tip. In **Figure 7A** the tip of a monomode fibre is cleaved at a specific angle and is subsequently coated with a metal layer of appropriate thickness. As the wave vector (cf. Eqn [2]) of the propagating light in a monomode fibre is well defined the cleaving angle can be calculated such that excitation of SPs is possible in the ε_a region of interest. Again, SP excitation is detected by a decreased reflected intensity. In order to obtain optimum response it is advisable to use polarization-preserving fibres. In **Figure 7B** another approach is depicted, involving the use of a multimode fibre. Here, the circumference of the tip is metal coated; additionally a mirror is deposited on the distal end to minimize reflection losses. For a multimode fibre a (discrete) range of wave vectors simultaneously propagates; in order to be able to detect changing characteristics of the metal/dielectric interface it is therefore necessary to use a broadband light source. The SPR information will now be contained in the wavelength-dependent reflectance. An advantage over the monomode configuration is that a broader range of SP wavevectors can be excited.

SPR microscopy

The foregoing discussion has ignored the possibility to obtain spatially resolved information from a SPR experiment. However, it is known that SPs are collective electron oscillations *with a limited coherence length* L_x, implying that two regions in the metal with a mutual distance larger than L_x are capable of supporting SPs which are mutually independent. This phenomenon can be exploited to image structures on top of a metal layer that have a distribution of different ε_a: if the angle of light incidence is such that one particular ε_a corresponds to resonance, then regions with another ε_a will exhibit larger reflectance. An example of such an experiment can be seen in **Figure 8**, where the spatially resolved reflectance of an inhomogeneous monomolecular layer, consisting of molecules oriented either tilted or perpendicularly to the surface is depicted.

Of course, in such an experiment one aims to obtain maximum lateral resolution, while retaining the vertical (thickness) resolution. A general rule is that L_x decreases for increasing resonance halfwidths (cf. **Figure 1C**). However, as was pointed out in an

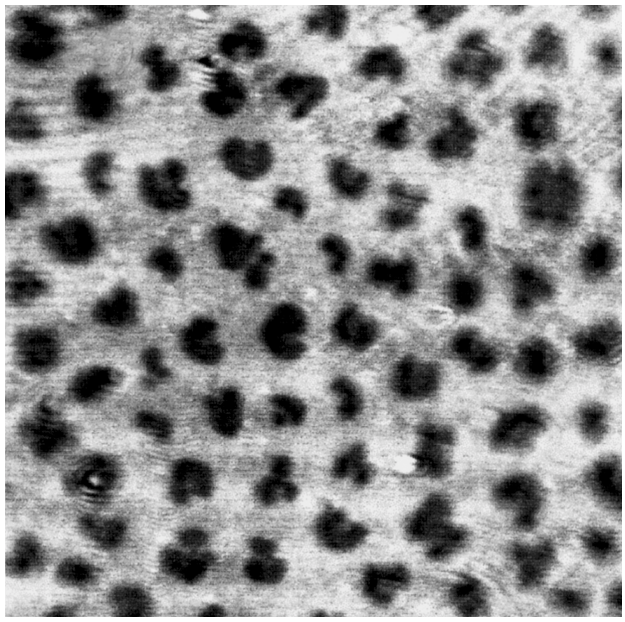

Figure 8 SP microscopic image of an inhomogeneous monolayer. Dimensions of image 0.2×0.2 mm^2. Thickness difference of the two types of domains is less than 0.4 nm. Lateral resolution approximately 3 μm.

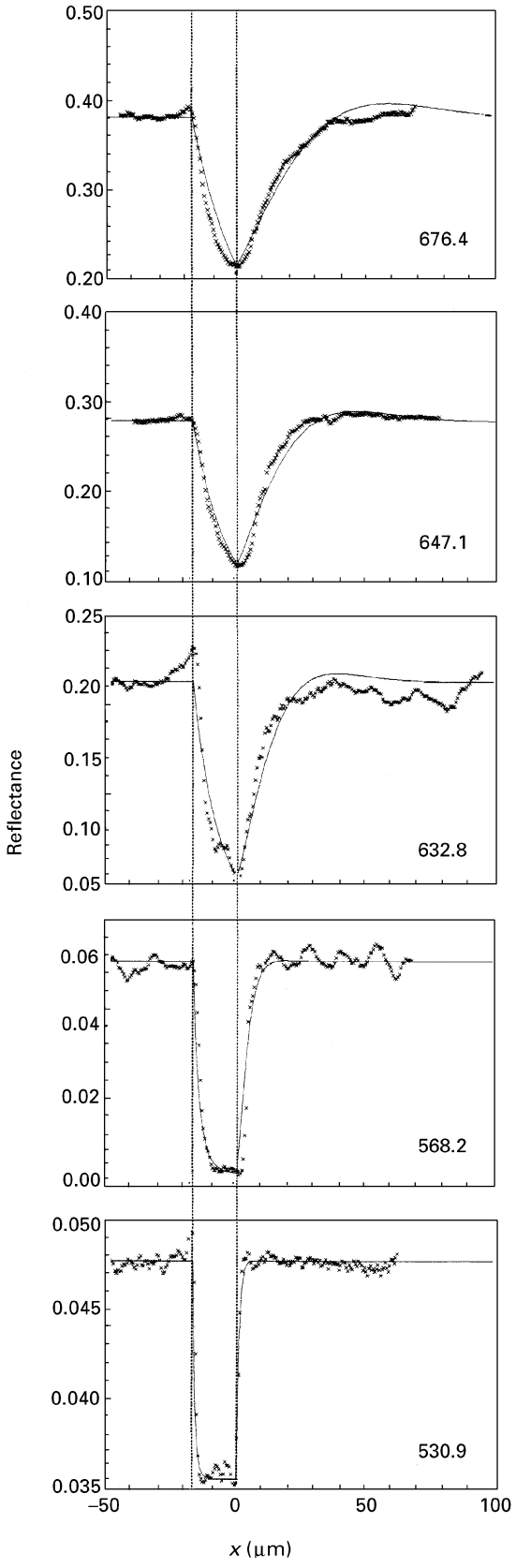

Figure 9 Lateral resolution in SPR microscopy. The vertical lines denote the physical width of a 2.5 nm SiO_2 ridge. Number insets correspond to the various wavelengths used.

earlier section, such an increasing SPR halfwidth simultaneously deteriorates vertical resolution. Therefore, for each particular situation a balance has to be sought between these two contradictory conditions. This is exemplified in **Figure 9** where SPR results are shown of a 2.5 nm SiO_2 ridge on gold for various wavelengths. It is clearly seen that at the shortest wavelength used the lateral resolution is the highest (~ 2 μm), but the slope is the lowest (compare also **Figure 2**), indicating that it is difficult to obtain sufficient intensity contrast to detect sub nm height differences, which is usually not a problem with standard SPR experiments.

Instrumentation

The first SPR microscopy experiments were done using a scanning focused beam. However, a straightforward approach, by imaging a collimated beam, proved to be much faster and instrumentally much simpler while at both the lateral and vertical resolution are comparable or better. Therefore, only this last approach will be discussed in more detail.

Figure 10 gives an overview of a representative setup. A prism/gold layer assembly and an optional cuvet system are placed on a rotation stage (angular increments 0.01 degree). SPs can be excited using light from a HeNe or an argon/krypton ion laser. This last light source has the advantage of providing a large number of high power wavelengths over the whole visible range. After having passed through a Pockels cell and a spatial filter, the light spot

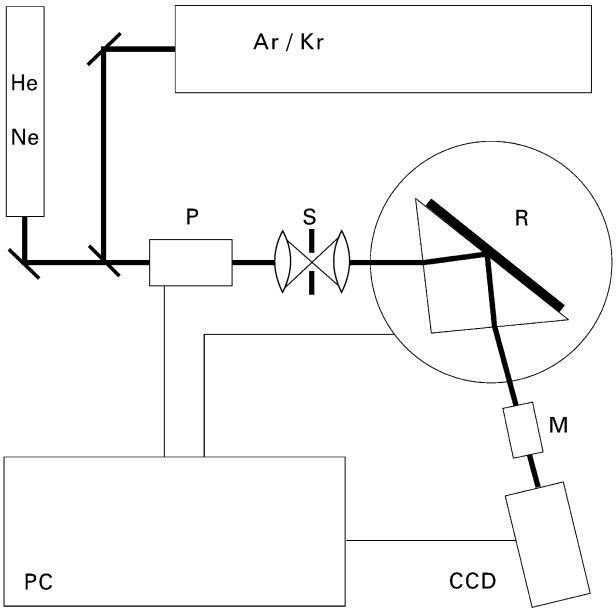

Figure 10 SPR microscope setup. P: Pockels cell; S: spatial filter; R: rotation stage; M: objective; CCD: video camera.

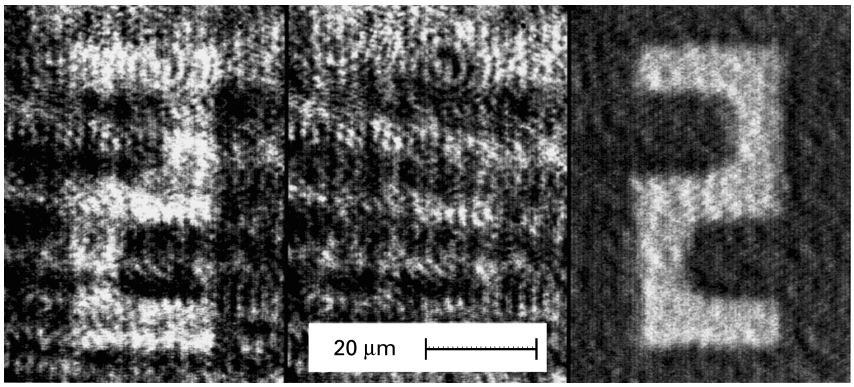

Figure 11 Improvement of image quality by dividing s- and p-polarized responses. From left to right: p response; s response; p/s response.

entering the prism has an area of ~1 cm^2. The intensity profile of the reflected beam is recorded with a microscope consisting of an objective and CCD video camera. It is important that the video camera has a response linear in the light intensity (see below). Depending on the light intensity and required magnification, objectives with focal distances between 5 and 50 mm are used. The Pockels cell and rotation stage are controlled by a microcomputer and the obtained images are also stored in this same computer by using a frame-grabber card.

It also proves possible to use the aforementioned gratings in a SPR microscopic experiment. Rotation of such a plate about the normal is equivalent to changing the angle of incidence of the exciting light. Compared to the standard prism setup this configuration is very compact and can easily be integrated in a conventional light microscope.

Improvement of image quality

Apart from the diffraction limit of the use of imaging lens there are a number of factors determining the eventual quality of a SPR microscopy image. As already mentioned, the use of shorter wavelengths generally improves lateral resolution, but simultaneously results in lower intensity contrasts for a given height difference. With such relatively low contrasts the use of a digital frame-grabber (which has a typical dynamic range of 2^8) can result in *quantization effects during image acquisition*, which become apparent if a low-contrast image is digitally amplified. To avoid this effect an option is to add a number of images with an effective dynamic range substantially larger than that of the frame-grabber used.

Integrating a number of images also results in averaging. This can be particularly important if shot noise is present when working with low light levels. Such an averaging will result in a signal-to-noise (SNR) improvement with a factor of $n^{1/2}$ where n is the number of added images. Another possible way to increase SNR is to increase laser power but this option is of limited value in view of the resulting destructive heating effects on the sample.

Another experimental problem is *lateral nonhomogeneity of the incoming laser beam intensity profile*. This can be partially solved by spatial filtering as indicated in **Figure 10**; however, if there are any unwanted, spurious reflections in the light path between the spatial filter and CCD camera, then again a beam nonhomogeneity will occur owing to the relatively large coherence length of the laser light used. An appropriate method is the use of a Pockels cell with simultaneous digital image processing. Such a cell can be configured such that the application of a voltage results in transmission of either p- or s-polarized light, without moving any part in the light beam. In the SPR microscope the Pockels cell is employed to acquire two images using p- and s-polarized light, respectively. The image with p-polarization contains the SPR microscopic image together with the contrast generated by spatial nonhomogeneities, whereas the image obtained with s-polarization only contains the same unwanted nonhomogeneities. Because the CCD camera output is linear in intensity, the ratio of the two images is a true representation of the SPR-related reflectance variations over the imaged surface. An example of the result of such an approach can be seen in **Figure 11**. Although lateral nonhomogeneities are still visible in the ratioed SPR image, the resolution is approximately 2 μm; for this image the difference in reflectance between the two regions is ~0.01.

Combination with other microscopies

Since the birth of scanning probe microscopy several attempts have been undertaken to merge this

approach with SP microscopy. In **Figure 12** a schematic diagram is given where a SPR microscope is combined with a scanning tunnelling microscope (STM). The hemisphere, serving as a prism, is metal-coated, and SPs are excited in the usual way. The metallic STM tip is brought close to the surface (distance ~5 nm). The area of interaction between the tip and the surface is imaged on a photodiode. The tip is allowed to scan laterally over the surface and the photodiode output is monitored simultaneously. It was found that small corrugations on the surface which were detected by the tunnelling current of the STM were equally well monitored by the SPR reflectance. In this way a lateral resolution of ~5 nm could be demonstrated *in a SPR image*. Similar conclusions could be made for a dielectric atomic force microscopy (AFM) tip. Even better results can be obtained if the conically scattered SPR radiation is monitored rather than the specularly reflected light.

A discussion on the contrast mechanism in both setups is far beyond the scope of the present article; a pragmatic remark is that, in most cases, an AFM type tip is preferable in view of the fact that in the latter case no conductivity conditions have to be imposed on the samples of interest.

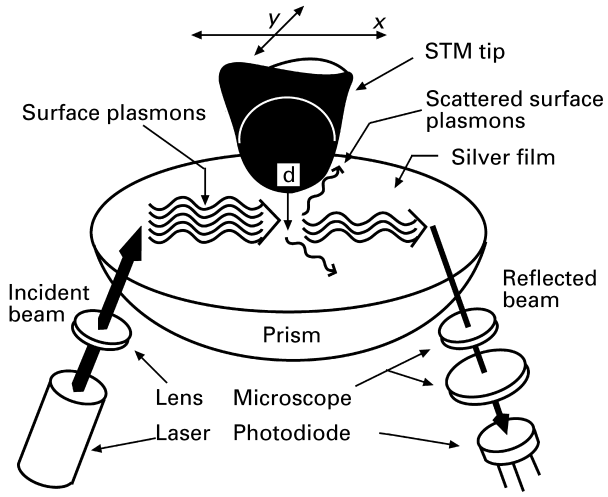

Figure 12 Scheme of a combined SP microscope and a scanning probe microscope. The tip can either be a STM or an AFM tip. Reproduced with permission from Specht M (1992) *Physical Review Letters* **68**: 476–479. American Physical Society.

List of symbols

k_x = wave vector; L_x = coherence length; n = refractive index; n = number of added images; R = reflectance; Δt = time span; ε = dielectric constant; λ = wavelength *in vacuo*; θ = angle of light; θ_{SPR} = angle of minimum reflectance.

See also: **Fibre Optic Probes in Optical Spectroscopy: Clinical Applications; Fourier Transformation and Sampling Theory; Light Sources and Optics; Photoacoustic Spectroscopy, Applications; Photoacoustic Spectroscopy, Theory; Scanning Probe Microscopes; Scanning Probe Microscopy, Applications; Scanning Probe Microscopy, Theory; Surface Plasmon Resonance, Applications; Surface Plasmon Resonance, Theory.**

Further reading

Agranovich VM and Maradudin AA (1982) *Surface Polaritons*. Amsterdam: North-Holland Publishing Company.

Kretschmann E (1971) Die bestimmungen optischer Konstanten von Metallen durch Anregung von Oberflächen plasmaschwingungen. *Zeitschrift Physica* **241**: 313–321.

Lawrence CR and Geddes NJ (1997) SPR for Biosensing. In: Kress-Rogers E (ed) *Handbook of Biosensors and Electronic Noses*. Boca Rata, FL: CRC Press.

Raether H (1988) *Surface Plasmons on Smooth and Rough Surfaces and on Gratings*. Berlin: Springer Verlag.

Rothenhäusler B and Knoll W (1988) Surface plasmon microscopy. *Nature* **332**: 615–616.

Specht M, Pedarnig JD, Heckl M, and Hansch TW (1992) Scanning plasmon near-field microscope. *Physical Review Letters* **68**: 476–478.